Mineralogical Magazine, August 2018, Vol. 82(4), pp. 913–928

Oxy-dravite from Wołowa Góra Mountain, Karkonosze massif, SW Poland: Crystallochemical and structural studies

Adam Pieczka[1,*], Andreas Ertl[2,3], Mateusz P. Sęk[1], Diana Twardak[1], Sylwia Zelek[1], Eligiusz Szełęg[4] and Gerald Giester[3]

[1] AGH University of Science and Technology, Department of Mineralogy, Petrography and Geochemistry, al. Mickiewicza 30, 30-059 Kraków, Poland
[2] Mineralogisch-Petrographische Abt., Naturhistorisches Museum, Burgring 7, 1010 Wien, Austria
[3] Institut für Mineralogie und Kristallographie, Geozentrum, Universität Wien, Althanstrasse 14, A-1090 Wien, Austria
[4] University of Silesia, Faculty of Earth Sciences, Department of Geochemistry, Mineralogy and Petrography, 41-200 Sosnowiec, Będzińska 60, Poland

[*Received 4 July 2017; Accepted 5 September 2017; Associate Editor: Mark Welch*]

ABSTRACT

Yellowish dravitic tourmaline (dominated by the oxy-dravite component) associated with secondary fluor-dravite/fluor-schorl and dravite/schorl tourmalines was found in a quartz vein cropping out in the eastern part of the Karkonosze Mountains range, SW Poland. The crystal structure of this tourmaline was refined to an R_1 value of 1.85% based on single-crystal data, and the chemical composition was determined by electron-microprobe analysis. The tourmaline, a representative of the alkali-tourmaline group, has the structural formula: $(Na_{0.75}Ca_{0.12}\square_{0.13})_{\Sigma1}(Mg_{1.93}Al_{0.95}Ti_{0.06}Fe^{2+}_{0.04}V_{0.01})_{\Sigma3}(Al_{5.38}Mg_{0.62})_{\Sigma6}B_3Si_6O_{27}(OH)_3(O_{0.46}OH_{0.33}F_{0.21})_{\Sigma1}$, and is characterized by an extremely high Mg/(Mg + Fe) ratio of 0.97–0.99, the $^{W}O^{2-}$ content that reaches 0.59 apfu resulting in a local predominance of the oxy-dravitic component and Mg–Al disorder on the octahedral *Y* and *Z* sites of the order of 0.64 apfu. This disordering results in an increasing <*Z*–O> distance with ~1.925 Å, and unit-cell parameters $a = 15.916(1)$ Å and $c = 7.180(1)$ Å. The tourmaline formed during Variscan prograde metamorphism under the influence of a released (H_2O,B,F)-bearing fluid. The fluid mobilized the most soluble components of partly altered silicic volcaniclastic material of the Late Cambrian to Early Ordovician bimodal volcanism to become the protolith for adjacent quartzo-feldspathic schists and amphibolites, and propagated them into the surrounding granitic gneisses of the Kowary unit in the eastern metamorphic cover of the Karkonosze granite.

Keywords: dravitic tourmaline, oxy-dravite, fluor-dravite, dravite, chemical composition, crystal structure, order-disorder.

Introduction

Minerals of the tourmaline supergroup are common accessory phases occurring in numerous igneous, metamorphic and sedimentary rocks. They are complex borosilicates with compositions corresponding to the generalized chemical formula $XY_3Z_6(T_6O_{18})(BO_3)_3V_3W$ (Henry *et al.*, 2011), where *X*, *Y*, *Z*, *T*, *B*, *V* (=O3) and *W* (=O1) denote structural sites occupied as follows.

$$X = Na^+, K^+, Ca^{2+}, Pb^{2+}, \square \text{ (vacancy)};$$

$$Y = Fe^{2+}, Mg^{2+}, Mn^{2+}, Al^{3+}, Li^+, Fe^{3+}, Zn^{2+}, Cr^{3+}, V^{3+}, Ti^{4+}, Cu^{2+}, Ni^{2+}, \ldots;$$

*E-mail: pieczka@agh.edu.pl
https://doi.org/10.1180/minmag.2017.081.069

$Z = Al^{3+}, Mg^{2+}, Fe^{3+}, Cr^{3+}, V^{3+}, ...;$

$T = Si^{4+}, Al^{3+}, B^{3+};$

$B = B^{3+};$

$V = OH^{-}, O^{2-};$ and

$W = OH^{-}, F^{-}, O^{2-}.$

The extremely complex chemical composition results in numerous colour varieties, sometimes showing gem-quality features, although the most common Fe-bearing crystals are usually dark-brown to black.

In Poland, occurrences of tourmaline-supergroup minerals are generally limited to metamorphic and igneous rocks of the Sudetes region and crystalline rocks of the Tatra Mountains (Pieczka, 1996; Gawęda *et al*., 2002). Tourmalines in those areas are mainly very dark green to black Fe-bearing species, mainly schorl. The Góry Sowie Block is the only geological unit in Poland known for occurrences of multicoloured Li-bearing tourmalines, where they may be found in LCT-type pegmatites, e.g. in the vicinity of Gilów (Pieczka *et al*., 2004) and Piława Górna (Pieczka *et al*., 2010). Additionally, a dark blue dravite was described from a small lens of a LCT-type pegmatite hosted by serpentinite of the Szklary massif (Pieczka, 2007), considered to be an external representative of the Góry Sowie pegmatitic melts intruded into ultrabasic rocks of the Sudetic ophiolite before ~380 Ma (Pieczka *et al*., 2015).

In addition to the Góry Sowie area, Wołowa Mountain in the eastern part of Karkonosze Mountains is the only locality in the Polish part of the Sudetes with occurrences of schorlitic to dravitic tourmalines, varying in colour from black through olive-green to yellow (Lis *et al*., 1965). Pieczka (1996) gives brief details of Fe-bearing tourmalines from the locality; in the present paper we describe the yellowish dravitic tourmaline in term of its crystal chemistry and structure. Oxy-dravite tourmaline, the end-member species usually dominant in the dravitic tourmaline studied, was mentioned in the tourmaline classification proposal of Hawthorne and Henry (1999). Subsequently the term was used in the classification of Mg- and Al-bearing tourmalines with the O^{2-}-dominant *W* site, and recently it was approved by the International Mineralogical Association Commission on New Minerals, Nomenclature and Classification as a valid mineral of the tourmaline supergroup (Bosi and Skogby, 2012, 2013). Occasionally it occurs in rocks of Cr- and V-rich environments. Such tourmaline species can be enriched in V and Cr, and sometimes also in Fe^{3+}. These elements can even be the dominant occupants at the *Y* site and/or *Z* site, e.g. in oxy-vanadium-dravite (Bosi *et al*., 2013*a*), originally described as 'vanadium-dravite' by Reznitsky *et al*. (2001), oxy-chromium-dravite, vanadio-oxy-dravite, vanadio-oxy-chromium-dravite, chromo-alumino-povondraite (Baksheev *et al*., 2011; Bosi *et al*., 2012; 2013*b*; 2014*a*,*b*; 2017; Reznitskij *et al*. 2014) and bosiite (Ertl *et al*., 2016). The Wołowa Mountain tourmaline, however, features a relatively simple chemistry with negligible V and Cr, and probably absent Fe^{3+}, which reflects the chemistry of the environment in which the tourmaline grew.

Occurrence

The Karkonosze granite massif is the largest Variscan pluton in the Western Sudetes at the northeastern margin of the Bohemian Massif, hosted by the Izera Metamorphic Complex on the northwest, and the South Karkonosze Metamorphic Unit, the East Karkonosze Metamorphic Unit and the Kaczawa Metamorphic Complex on the northeast (Fig. 1). The East Karkonosze Metamorphic Unit comprises the Kowary–Czarnów Unit divided into the Kowary gneiss series and the Czarnów schist series and the Leszczyniec Unit (Mazur *et al*., 2007). The Kowary gneiss series, which contacts the granite, is composed of gneisses, mica-schists, amphibolites, phyllites and marbles (*ibid.*). The region of Wołowa Góra Mountain located ~3 km SW from Kowary, marks the NE termination of the Karkonosze montane range and is the SW part of the East Karkonosze Metamorphic Unit in Poland. The region is composed mainly of leucocratic augen gneisses associated with granitic gneisses and subordinate layered gneisses of the Kowary gneiss series, surrounded on the south and west by an assemblage of chlorite-mica schists, quartzo-feldspathic schists and amphibolites, formed from differentiated igneous and volcanogenic–sedimentary ~500 Ma protoliths (Berg, 1923; Lis *et al*., 1965; Różański, 1995; Oberc-Dziedzic *et al*., 2010). A pass between Wołowa Mountain and Czoło Mountain in the main Karkonosze range is the well-known locality of a milky quartz vein with brannerite, associated with tourmalines showing colours varying from black, found in the host

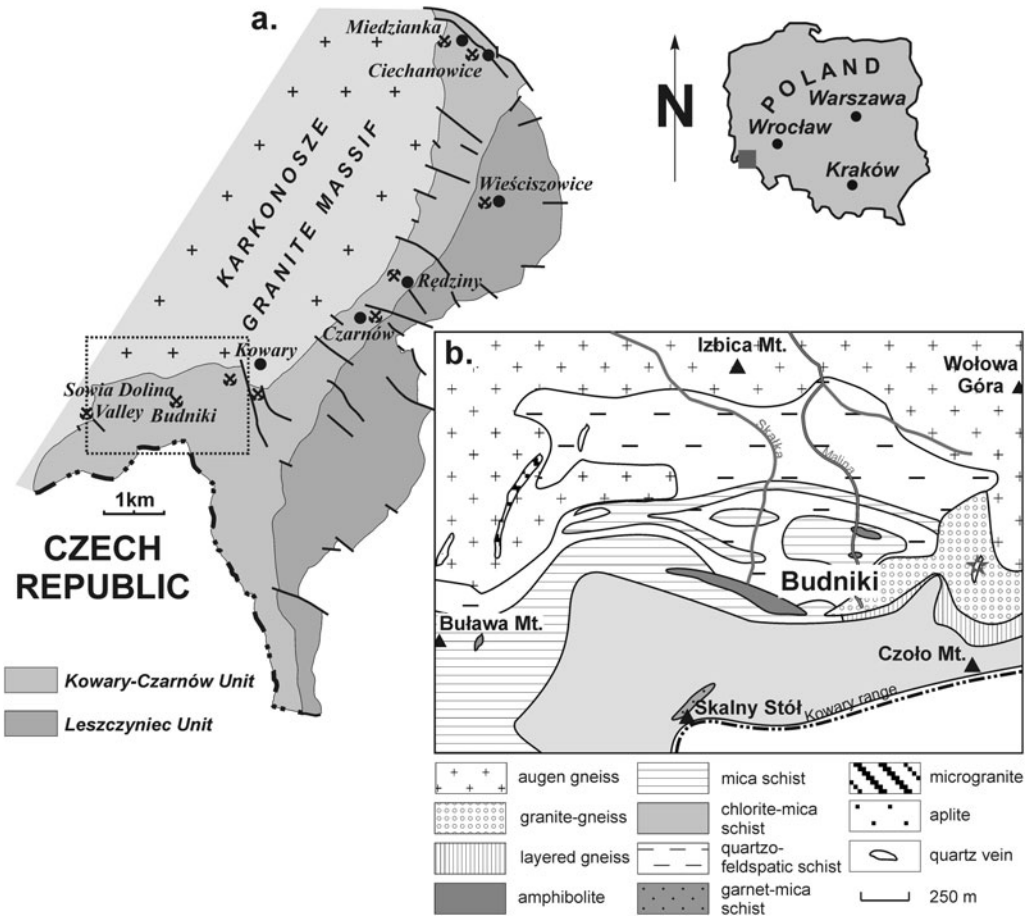

FIG. 1. (*a*) Geological sketch of the East Karkonosze Metamorphic Unit (after Pieczka *et al*., 2009). (b) Detailed geological map of the Budniki–Wołowa Mountain region (after Różański, 1995; *fide* Mochnacka *et al*., 2008) shown as a black dotted frame in (a). The occurrence of the quartz vein with dravitic tourmaline is marked by a grey star.

granitic gneisses, through olive-green to yellow in the quartz vein itself (Lis *et al*., 1965). The surrounding granitic gneisses are medium- to coarsely-crystalline, light-pinkish rocks composed of microcline, microcline perthite, quartz and pale-coloured mica, with strong albitization, which almost completely altered the primary K-feldspars, leading commonly to the formation of chessboard-twinned albite. The contact between the host granitic gneisses and the quartz vein is some metres long and 5–50 cm thick emphasized by the presence of altered dark micas and dark green tourmaline. The tourmaline occurs as radial aggregates, a few centimetres thick, composed of elongated, prismatic crystals (Lis *et al*., 1965; Pieczka, 1996), which become pale green inside the vein, reaching a yellowish coloration in its axial part. Brannerite, gersdorffite, pale-coloured micas, an apatite-group mineral, pyrite, pharmacosiderite and Fe oxides were recognized as the associated minerals (Lis *et al*., 1965).

Methods

Electron microprobe analysis (EMPA)

Electron microprobe analyses were performed at the Inter-Institute Analytical Complex for Minerals and Synthetic Substances at the University of Warsaw on a longitudinal section of an aggregate composed of yellowish tourmaline crystals, using a Cameca SX 100 electron microprobe operating in wavelength-dispersive mode under the following conditions: accelerating voltage of 15 kV, beam

current of 20 nA, beam diameter of 2 μm, peak count-time of 20 s and background time of 10 s. Standards, diffracting crystals, analytical lines, and mean detection limits (in wt.%) were as follows: phlogophite – F (TAP, *K*α, 0.17), albite – Na (TAP, *K*α, 0.02), diopside – Mg (TAP, *K*α, 0.02), Si (TAP, *K*α, 0.02) and Ca (PET, *K*α, 0.02), orthoclase – Al (TAP, *K*α, 0.02) and K (PET, *K*α, 0.02), rutile – Ti (PET, *K*α, 0.02), rhodonite – Mn (LIF, *K*α, 0.06), hematite – Fe (LIF, *K*α, 0.06), V_2O_5 – V (LIF, *K*α, 0.03), Cr_2O_3 – Cr (LPET, *K*α, 0.04) and sphalerite – Zn (LIF, *K*α, 0.09). The raw data were reduced with the 'PAP' routine of Pouchou and Pichoir (1985).

Atomic fractions for crystallochemical formulae were normalized on the basis of: (1) 15 $Y+Z+T$ atoms per formula unit (apfu) or (2) $Y+Z=9$ apfu for cases where large amounts of SiO_2 where present, probably due to tiny inclusions of quartz on the micro- to nano-scale, with the assumed maximum Si content = 6 apfu. B_2O_3 was calculated assuming B = 3 apfu, and H_2O, occurring as OH groups, by stoichiometry based on electroneutrality of the formulae. Table 1 gives statistics for the compositional data for the three distinguished tourmaline varieties: (1) primary tourmaline of the first generation; (2) secondary tourmaline from transverse veinlets (generation 2a); and (3) secondary tourmaline from crystals terminations in the fissures filled with quartz (generation 2b). Representative compositions of the tourmalines are given in Table 2.

Crystal-structure refinement

The crystal structure of yellowish Mg-rich tourmaline was refined at the Institut für Mineralogie und Kristallographie, Geozentrum, Universität Wien, Austria. Firstly, the quality of different tourmaline crystals was checked with a Bruker APEXII diffractometer equipped with a CCD area detector and an Incoatec Microfocus Source IμS (30 W, multilayer mirror and Mo*K*α). The crystal with the best quality was subsequently measured on this diffractometer. Single-crystal X-ray diffraction data, up to 80°2θ, were collected at room temperature, integrated and corrected for Lorentz and polarization factors with an absorption correction by evaluation of partial multiscans. The structure was refined with *SHELXL97* (Sheldrick, 2008) using scattering factors for neutral atoms and a tourmaline starting model from Ertl *et al*. (2010) (sample R6b). Refinement was performed with anisotropic displacement parameters for all non-hydrogen atoms. Crystal data and details of the structure refinement are provided in Table 3. The various site occupancies were refined according to well-known characteristics of the tourmaline structure, and with guidance from the EMP analysis; this strategy appears sound with the resulting empirical formula being compatible with that determined from the EMP results. Magnesium and Fe were refined at the *Y* site, Si was fixed at the *T* site. The *X* site was refined by setting the Ca occupancy to 0.12 apfu allowing the remainder of the site to refine as Na = (0.88 – □) apfu. The occupancy of the *Z* site was fixed at $(Al_{893}Mg_{0.107})$; the ^{Z}Mg content was estimated due to the enlarged <*Z*–O> distance. The occupancy of the O1 site was fixed at $(O_{0.79}F_{0.21})$, based on chemical data. The occupancy of the H1 and H3 sites were fixed at 0.33 and 1.00, respectively, based on chemical data. The positions of the H atoms bonded to the oxygen at the O1 and O3 positions in the structure were taken from the difference-Fourier map and incorporated into the refinement model; the O1–H1 and O3–H3 bond lengths were constrained to be 0.97(3) Å. The refinement converged at a $R_1(F)$ value of 1.85% (Table 3). In Table 4, the atomic parameters and equivalent isotropic displacement parameters are listed, and in Table 5 selected interatomic distances in the refined tourmaline are presented. The crystallographic information file has been deposited with the Principal Editor of *Mineralogical Magazine* and is available as Supplementary material (see below).

Results and discussion

Compositional data

The sample of yellowish tourmaline was collected in the year 2000 from remnants of the quartz vein cropping out on the pass between Wołowa Mountain and Czoło Mountain in the main Karkonosze range. The prismatic, yellowish crystals reach 1.5–2.0 cm in length and 2–3 mm in diameter; they are colourless in thin section, with birefringence Δ ≈ 0.015–0.017 (Fig. 2). In places, the crystals are cross-cut by fissures filled with a secondary tourmaline or the host quartz. The crystal terminations in the fissures on the border with quartz are distinctly darker in hand specimens, yellowish-olive-brown, with Δ ≈ 0.023–0.025 (Fig. 3).

Statistics for the compositional data for the three distinguished tourmaline varieties are given in

TABLE 1. Statistics for compositions of dravitic tourmalines from Wołowa Góra Mountain.

	Primary tourmaline variety (Trm_i)* ($n = 21$)			Elongated zones in tourmaline (Trm_{ii}) ($n = 3$)			Crystal terminations in fissures (Trm_{iii}) ($n = 3$)		
	Range	Mean	SD	Range	Mean	SD	Range	Mean	SD
wt.%									
SiO_2	37.04–38.50	37.74	0.37	35.83–36.39	36.11	0.28	36.12–36.56	36.38	0.22
TiO_2	0.28–0.83	0.51	0.14	0.45–0.54	0.49	0.04	0.75–1.08	0.93	0.17
$B_2O_{3(calc.)}$	10.73–11.15	10.93	0.11	10.46–10.56	10.52	0.05	10.48–10.60	10.54	0.06
Al_2O_3	32.03–35.01	33.78	0.74	31.78–32.59	32.25	0.42	30.26–31.28	30.75	0.51
V_2O_3	bdl–0.43	0.11	0.09	bdl			bdl		
FeO	0.22–0.61	0.32	0.09	7.42–8.07	7.76	0.33	7.19–8.48	7.80	0.65
MgO	10.33–11.52	10.78	0.34	6.53–6.62	6.59	0.06	7.22–7.69	7.45	0.23
CaO	0.38–1.61	0.70	0.32	0.43–0.54	0.49	0.06	0.79–1.14	0.97	0.18
Na_2O	1.80–2.70	2.45	0.18	2.37–2.48	2.43	0.06	2.22–2.35	2.29	0.07
K_2O	bdl			0.02–0.05	0.03	0.02	0.02–0.07	0.04	0.02
$H_2O_{(calc.)}$	2.83–3.35	3.14	0.14	2.91–3.01	2.95	0.05	2.93–3.09	3.02	0.08
F	0.10–0.78	0.42	0.18	0.82–0.94	0.87	0.06	0.54–1.04	0.74	0.26
$–O=F_2$	−(0.33–0.04)	−0.18	0.07	−(0.39–0.35)	−0.37	0.02	−(0.44–0.23)	−0.31	0.11
Total	98.80–102.18	100.70	0.86	99.79–100.48	100.13	0.34	100.37–100.76	100.59	0.20
Atoms per formula unit									
Si^{4+}	6.00	6.00		5.95–5.99	5.97	0.02	5.99–6.00	6.00	0.01
Ti^{4+}	0.03–0.10	0.06	0.02	0.06–0.07	0.06	0.01	0.09–0.13	0.12	0.02
$B^{3+}_{(calc.)}$	3.00	3.00		3.00	3.00		3.00	3.00	
Al^{3+}	6.09–6.45	6.33	0.10	6.22–6.33	6.28	0.06	5.91–6.05	5.97	0.07
V^{3+}	bdl–0.05	0.01	0.01	bdl	0.00	0.00	bdl		
Fe^{2+}	0.03–0.08	0.04	0.01	1.02–1.12	1.07	0.05	0.99–1.18	1.07	0.10
Mg^{2+}	2.45–2.75	2.55	0.09	1.60–1.64	1.62	0.02	1.79–1.88	1.83	0.05
Ca^{2+}	0.07–0.28	0.12	0.06	0.08–0.10	0.09	0.01	0.14–0.20	0.17	0.03
Na^{+}	0.54–0.82	0.75	0.06	0.76–0.79	0.78	0.02	0.71–0.75	0.73	0.02
K^{+}	bdl			bdl–0.01	0.01	0.00	0.01	0.01	0.00
$O^{2–}$	27.31–27.59	27.46	0.08	27.23–27.33	27.29	0.05	27.25–27.43	27.29	0.03
$F^{–}$	0.05–0.40	0.21	0.09	0.43–0.49	0.46	0.03	0.28–0.54	0.39	0.14
$OH^{–}_{(calc.)}$	3.06–3.52	3.33	0.13	3.20–3.33	3.25	0.07	3.21–3.40	3.32	0.10

*SiO_2 for the tourmaline is assumed by stoichiometry to be equal to 6 apfu (see text).
(calc.) – calculated by stoichiometry (see text); *n* – number of analyses; SD – standard deviation.
Mn, Cr and Zn were below detection limit; bdl – content below detection limit.

TABLE 2. Representative compositions of dravitic tourmalines from Wołowa Góra Mountain.

n	Oxy-dravite 8	Fluor-dravite 7	Dravite 21
wt.%			
SiO_2	37.61	36.12	36.12
TiO_2	0.41	0.48	1.08
$B_2O_{3(calc.)}$	10.90	10.54	10.48
Al_2O_3	33.84	32.59	30.26
V_2O_3	0.21	bdl	bdl
FeO	0.27	7.42	8.48
MgO	10.62	6.62	7.22
CaO	0.89	0.43	1.14
Na_2O	2.59	2.48	2.22
K_2O	bdl	0.02	0.07
$H_2O_{(calc.)}$	3.06	2.91	3.05
F	0.30	0.94	0.64
$–O=F_2$	0.13	–0.39	–0.27
Total	100.57	100.14	100.49
apfu			
Na^+	0.80	0.79	0.71
K^+	0.00	0.00	0.01
Ca^{2+}	0.15	0.08	0.20
□	0.05	0.13	0.09
ΣX	1.00	1.00	1.00
Mg^{2+}	2.53	1.63	1.79
Fe^{2+}	0.04	1.02	1.18
Al^{3+}	6.36	6.29	5.90
V^{3+}	0.03	bdl	bdl
Ti^{4+}	0.05	0.06	0.13
Σ(Y + Z)	9.00	9.00	9.00
B^{3+}	3.00	3.00	3.00
Si^{4+}	6.00	5.96	5.99
Al^{3+}	bdl	0.04	0.01
ΣT	6.00	6.00	6.00
$O^{2–}$	27.59	27.32	27.29
$OH^–$	3.26	3.19	3.37
$F^–$	0.15	0.49	0.34

Notes: Mn, Cr and Zn are below detection limits; bdl – content below detection limit; *n* – number of analyses.

TABLE 3. Crystallographical data and refinement details for oxy-dravite from Wołowa Góra Mountain.

X-ray radiation	Mo$K\alpha$ ($\lambda = 0.71073$ Å)
Z	3
Space group	$R3m$ (no. 160)
a, c (Å)	15.916(1), 7.180(1)
V (Å^3)	1575.2(3)
Crystal dimensions (mm)	0.10 × 0.12 × 0.15
Collection mode, $2\theta_{max}$ (°)	full sphere, 79.97
Index ranges	$-28 \le h \le 28$ $-28 \le k \le 28$ $-12 \le l \le 12$
Total reflections measured	30,871
Unique reflections	2330 ($R_{int}^{\ddagger}$ 2.81%)
$R_1(F)$ *, $wR_2(F^2)^{\dagger}$	1.88%, 4.39%
Flack x parameter	0.047(59)
'Observed' refls. [$F_o > 4\sigma(F_o)$]	2323
Extinct. coefficient	0.00000(13)
No. of refined parameters	94
GooF§	1.160
$\Delta\rho_{min}$, $\Delta\rho_{max}$ (e^-/Å^3)	–0.38, 0.49

Note: multi-scan absorption correction; refinement on F^2. Frame width, scan time, detector distance: 3°, 240 s, 35 mm. Scan mode: sets of ϖ and θ scans.
$^*R_1 = \Sigma||F_o| - |F_c||/\Sigma|F_o|$
$^{\dagger}wR_2 = \{\Sigma[w(F_o^2 - F_c^2)^2]/\Sigma[w(F_o^2)^2]\}^{1/2}$
$w = 1/[\sigma^2(F_o^2) + (aP)^2 + bP]$, $P = [2F_c^2 + \mathrm{Max}(F_o^2,0)]/3$
$^{\ddagger}R_{int} = \Sigma|F_o^2 - F_o^2(\mathrm{mean})|/\Sigma[F_o^2]$
$^{\S}\mathrm{GooF} = S = \{\Sigma[w(F_o^2 - F_c^2)^2]/(n–p)\}^{1/2}$

Table 1 and representative analyses of the tourmalines in Table 2. The primary tourmaline (Trm_i) has high SiO_2 and MgO contents, ranging between 37.04–38.50 wt.% and 10.33–11.52 wt.%, respectively; rather moderate Al_2O_3 and Na_2O of 32.03–35.01 wt.% and 1.80–2.70 wt.%, accompanied by subordinate TiO_2 (0.28–0.83 wt.%), FeO (0.22–0.61 wt.%) and V_2O_3 (up to 0.43 wt.%). The amount of F ranges from 0.10 to 0.78 wt.%. In contrast, the secondary Fe-enriched tourmalines Trm_{ii} and Trm_{iii} have typical SiO_2 contents (35.83–36.39 and 36.12–36.56 wt.%, respectively), slightly decreased Al_2O_3 (31.78–32.59 and 30.26–31.28 wt.%) and Na_2O (2.37–2.48 and 2.22–2.35 wt.%), much higher than in the main tourmaline variety, but similar FeO (7.42–8.07 and 7.19–8.48 wt.%) and MgO (6.53–6.62 and 7.22–7.69 wt.%), increased TiO_2 (0.45–0.54 and 0.75–1.08 wt.%) and CaO (0.43–0.54 and 0.79–1.14 wt.%). Fluorine increases up to 0.82–0.94 wt.% in the Trm_{ii} tourmaline, and locally up to 1.04 wt.% in the Trm_{iii} variety. B_2O_3 and H_2O complete the analyses (10.46–10.56 wt.% and 2.91–3.01 wt.%, and 10.48–10.60 wt.% and 2.93–3.09 wt.%, respectively).

All three tourmalines have the *Y* sites dominated by Mg although to different degrees. The primary Trm_i tourmaline has very high values of the Mg/(Mg + Fe) ratio, of the order of 0.97–0.99; the remaining two tourmalines are similar to each other for this ratio with values of 0.59–0.61 and 0.60–0.66, respectively, but distinctly lower than those related to Trm_i. All tourmaline varieties are alkali-

TABLE 4. Atom parameters in oxy-dravite from Wołowa Góra Mountain.

Site	*x*	*y*	*z*	U_{eq}	Occupancy
X	0	0	0.2337(2)	0.0193(3)	$Na_{0.744(7)}Ca_{0.120}$
Y	0.12461(3)	½×	0.63230(7)	0.0062(1)	$Mg_{0.949(3)}Fe_{0.051(3)}$
Z	0.29786(2)	0.26151(2)	0.61170(5)	0.00440(5)	$Al_{0.893}Mg_{0.107}$
B	0.10983(4)	2×	0.4547(2)	0.0054(2)	$B_{1.00}$
T	0.19176(1)	0.18986(2)	0	0.00407(4)	$Si_{1.00}$
O1 (*W*)	0	0	0.7722(2)	0.0119(3)	$O_{0.79}F_{0.21}$
H1	0	0	0.907(3)	0.01426*	$H_{0.33}$
O2	0.06091(3)	2×	0.48589(14)	0.0102(2)	$O_{1.00}$
O3 (*V*)	0.26408(9)	½×	0.51079(14)	0.0121(2)	$O_{1.00}$
H3	0.261(2)	½×	0.383(2)	0.01457*	$H_{1.00}$
O4	0.09331(4)	2×	0.07100(14)	0.0092(1)	$O_{1.00}$
O5	0.18430(7)	½×	0.09273(13)	0.0092(1)	$O_{1.00}$
O6	0.19540(5)	0.18529(5)	0.77746(9)	0.0075(1)	$O_{1.00}$
O7	0.28507(4)	0.28484(4)	0.07927(9)	0.00728(9)	$O_{1.00}$
O8	0.20946(5)	0.27022(5)	0.44096(10)	0.0083(1)	$O_{1.00}$

Note: Definition for U_{eq} – see Fischer and Tillmanns (1988).
*Isotropic displacement parameters (U_{iso}) for H1 and H3 constrained to have a U_{iso} 1.2 times the U_{eq} value of the O1 and O3 oxygen atoms.

group tourmalines plotting close to the Na corner in the ternary system *X*-site vacancy – Na – Ca, with a spread of data along the Na–Ca side (Fig. 4*a*). The *W* site of Trm_i is partly occupied by O^{2-} (0.31–0.59 pfu), and partly by OH^- (0.06–0.52 apfu) and F^- (0.05–0.40 pfu), with varying proportions of bivalent $^{W}O^{2-}$ and monovalent $^{W}(OH + F)^-$ anions. Therefore, it only partly meets requirements for an oxy-species (oxy-dravite), whereas the hydroxy-species (dravite) with $^{W}(OH + F) > {}^{W}O$ and OH > F is more common (Fig. 4*b*). However, oxy-dravite is commonly the dominant end-member component in this tourmaline. Tourmaline from transverse veinlets cutting the crystals, Trm_{ii}, always has $^{W}(OH + F) > {}^{W}O$ and OH < F, thus is a fluor-species, whereas Trm_{iii} tourmaline, forming crystal terminations in fissures filled with quartz, always has $^{W}(OH + F) > {}^{W}O$ with varying OH and F amounts, and is a fluor-species grading to a hydroxy-species.

TABLE 5. Selected interatomic distances in oxy-dravite from Wołowa Góra Mountain.

X–O2 ×3	2.4697(14)	T–O7	1.6030(6)
X–O5 ×3	2.7345(11)	T–O6	1.6019(7)
X–O4 ×3	2.8250(12)	T–O4	1.6239(4)
<X–O>	2.676(1)	T–O5	1.6405(5)
		<T–O>	1.6173(6)
Y–O1	1.9895(10)		
Y–O6 ×2	1.9955(7)		
Y–O2 ×2	1.9976(7)	B–O2	1.367(2)
Y–O3	2.1112(12)	B–O8 (×2)	1.3769(9)
<Y–O>	2.0145(8)	<B–O>	1.374(1)
Z–O6	1.8892(7)	O1–H1	0.97(2)
Z–O8	1.8920(7)	O3–H3	0.92(2)
Z–O7	1.9005(7)		
Z–O8’	1.9227(7)		
Z–O7’	1.9556(7)		
Z–O3	1.9880(5)		
<Z–O>	1.9247(7)		

FIG. 2. A fragment of the quartz vein from Wołowa Góra Mountain with yellowish oxy-dravite tourmaline (scale bar = 2 cm).

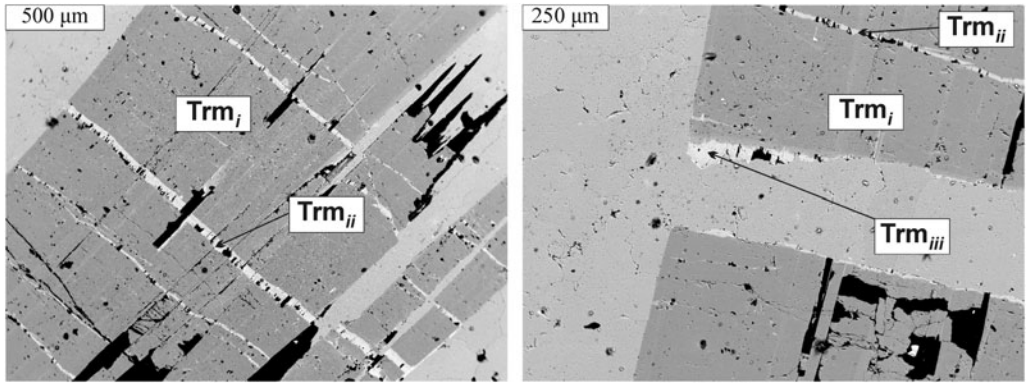

FIG. 3. Back-scattered electron images of yellowish tourmaline from Wołowa Góra Mountain Abbreviations: Trm$_i$ – primary tourmaline (oxy-dravite), Trm$_{ii}$ – secondary tourmaline crystallizing in close transversal veinlets (fluor-dravite), Trm$_{iii}$ – secondary tourmaline crystallizing in open fissures as crystals terminations (dravite), later filled by quartz.

The covariation between Al and Mg + Fe as the main components at the octahedral *Y* and *Z* sites is presented in Fig. 5*a*. A strong negative linear relationship ($r^2 = 0.96$) corroborates the dominant role of one of the typical tourmaline-supergroup substitutions of deprotonation type, $Mg(Fe)^{2+} + (F, OH)^- \rightarrow Al^{3+} + O^{2-}$, and an insignificant role of the second possible substitution of alkali-vacancy type, $Na^+ + Mg(Fe)^{2+} \rightarrow \square + Al^{3+}$, due to the almost similar *X*-site vacancies, 0.13, 0.13 and 0.10 apfu on average in the Trm$_i$–Trm$_{iii}$ varieties, respectively. Along with textural relationships and Mg/(Mg + Fe) values of 0.97–0.99, it indicates that the oxy-species participating significantly in the composition of the primary tourmaline had been replaced by the secondary Fe-enriched fluor-tourmaline and hydroxy-tourmaline species, with the decreased Mg/(Mg + Fe) values. Additionally, increasing Fe is mainly a result of the simple isovalent substitution $Fe^{2+} \rightarrow Mg^{2+}$ ($r^2 = 0.94$; Fig. 5*b*), and not the substitution $Fe^{3+} \rightarrow Al^{3+}$ (Fig. 6). The latter has been well-documented, e.g. in the form of continuous solid-solution between end-members oxy-dravite and povondraite by Žáček *et al*. (2000).

The *X* site is mainly filled with Na; another *X*-site occupant is Ca or the site remains unfilled, i.e. occurs as vacancies. In the primary Trm$_i$ dravite, Ca displays a weak positive correlation with F ($r^2 = 0.47$) (Fig. 5*c*), which, at least partly indicates that the elevated ^{X}Ca contents can be a partial result of $Ca^{2+} + Mg(Fe)^{2+} + F^- \rightarrow {}^X Na^+ + {}^Z Al^{3+} + {}^W OH^-$ substitution, leading to the presence of end-member fluor-uvite, $CaMg_3(Al_5Mg)(Si_6O_{18})(BO_3)_3(OH)_3F$, and a hypothetical end-member fluor-feruvite, $CaFe_3^{2+}(Al_5Mg)(Si_6O_{18})(BO_3)_3(OH)_3F$. Successively, the *X*-site vacancy is a result of a simple substitution $\square + Al^{3+} \rightarrow {}^X Na^+ + {}^Y Mg(Fe)^{2+}$ of the foitite type, and indicates the compositional importance of the magnesio-foitite and foitite components, $Na(Mg_2Al)Al_6(Si_6O_{18})(BO_3)_3(OH)_3(OH)$ and $Na(Fe_2^{2+}Al)Al_6(Si_6O_{18})(BO_3)_3(OH)_3(OH)$, respectively, in compositions of the tourmalines.

Careful inspection of Fig. 6 indicates that the compositions of all the tourmaline varieties studied can be explained as complex solid-solutions of six end-member pairs: (dravite/schorl) + (fluor-dravite/fluor-schorl) + (oxy-dravite/oxy-schorl) + (magnesiofoitite/foitite) + (uvite/feruvite) + (fluor-uvite/fluor-feruvite). Although assigning hypothetical end-members to the compositions is strongly dependent on the order of species calculations, abundances of two of the pairs can be evaluated easily on the basis of the $^X\square$ and $^W O^{2-}$ contents (magnesiofoitite + foitite, and oxy-dravite + oxy-schorl, respectively). The results show that the composition of the primary yellowish tourmaline Trm$_i$, is dominated by the oxy-dravitic component (~31–59 mol.%), only yielding the components dravite or fluor-dravite in single analytical spots. Successively, the secondary tourmaline Trm$_{ii}$, with Mg only slightly exceeding Fe^{2+}, Al close to 6 apfu and $^W F > {}^W OH \approx {}^W O^{2-}$ is always dominated by fluor-dravite + fluor-schorl, whereas Trm$_{iii}$ fluctuates between dravite + schorl and fluor-dravite + fluor-schorl. The abundance of oxy-dravite + oxy-schorl components decreases from the main tourmaline variety, where the species dominate, down to tourmaline forming transverse veinlets and finally to tourmaline on terminations

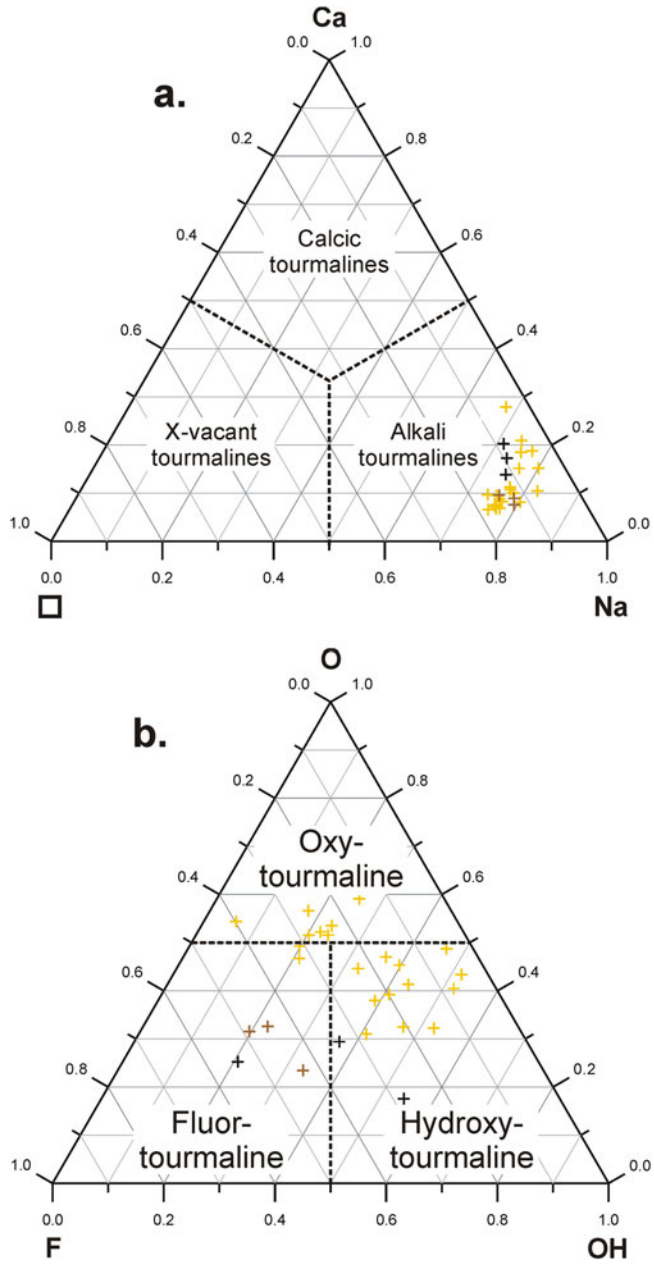

FIG. 4. Classification of tourmalines from Wołowa Góra Mountain in term of: (*a*) *X*-site occupants; and (*b*) *W*-site occupants. Symbols: yellow crosses – Trm_{i}, the primary tourmaline; brown crosses – Trm_{ii}, tourmaline from transverse veinlets; black crosses – Trm_{iii}, tourmaline from the crystal terminations in fissures.

of crystals in open fissures. In contrast, the abundance of dravite + schorl components increases in the opposite direction, with an episode of dominance of fluor-dravite + fluor-schorl during crystallization in transverse fissures within crystals of the primary dravite.

Hawthorne (1996) presented an explanation for the presence of O^{2-} at the *W* site of the tourmaline

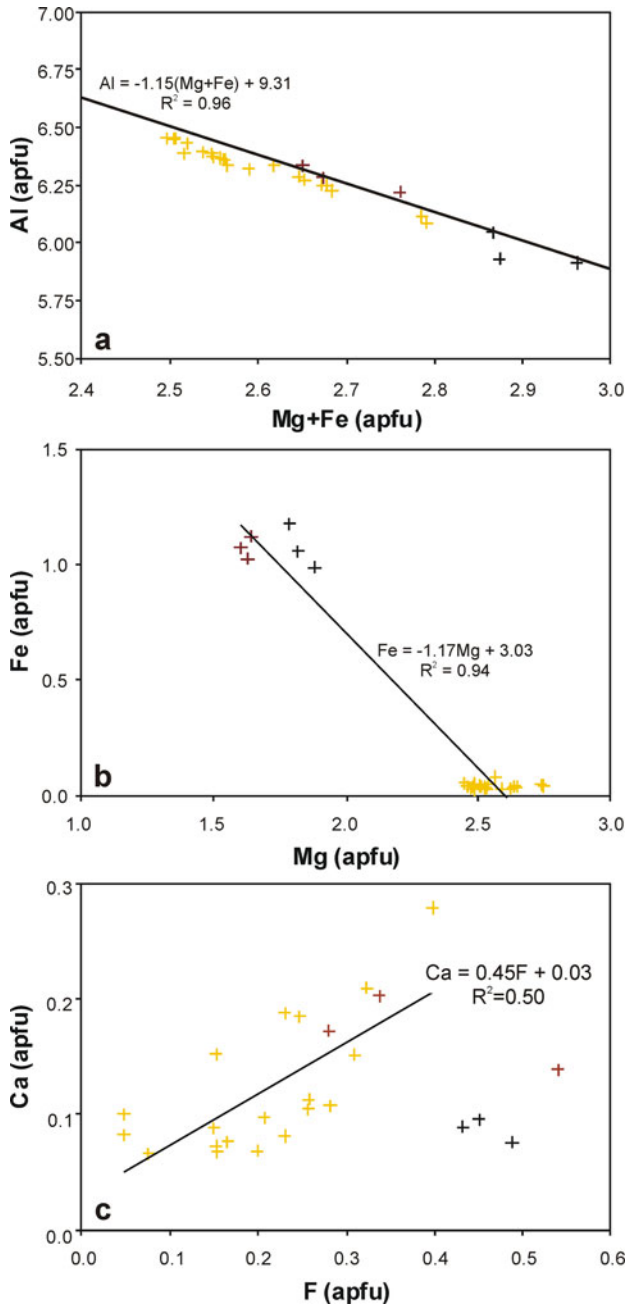

FIG. 5. Compositional relationships in the Wołowa Góra Mountain tourmalines: (*a*) Al *vs.* Mg + Fe, (*b*) Fe *vs.* Mg, (*c*) Ca *vs.* F covariation. Symbols as in Fig. 4.

structure, a characteristic feature of oxy-dravite, which can be satisfied for 3Al or 2Al + Mg local arrangements of the *Y*-octahedra triad. This requirement can be fulfilled by Mg–Al disorder induced through the substitution $^{W}(OH)^{-} + {}^{Y}Mg_2 + {}^{Z}Al \leftrightarrow {}^{W}O^{2-} + {}^{Y}Al_2 + {}^{Z}Mg$, leading to the end-member oxy-dravite, $Na(Al_2Mg)(Al_5Mg)(Si_6O_{18})(BO_3)_3(OH)_3O = NaAl_3(Al_4Mg_2)(Si_6O_{18})$

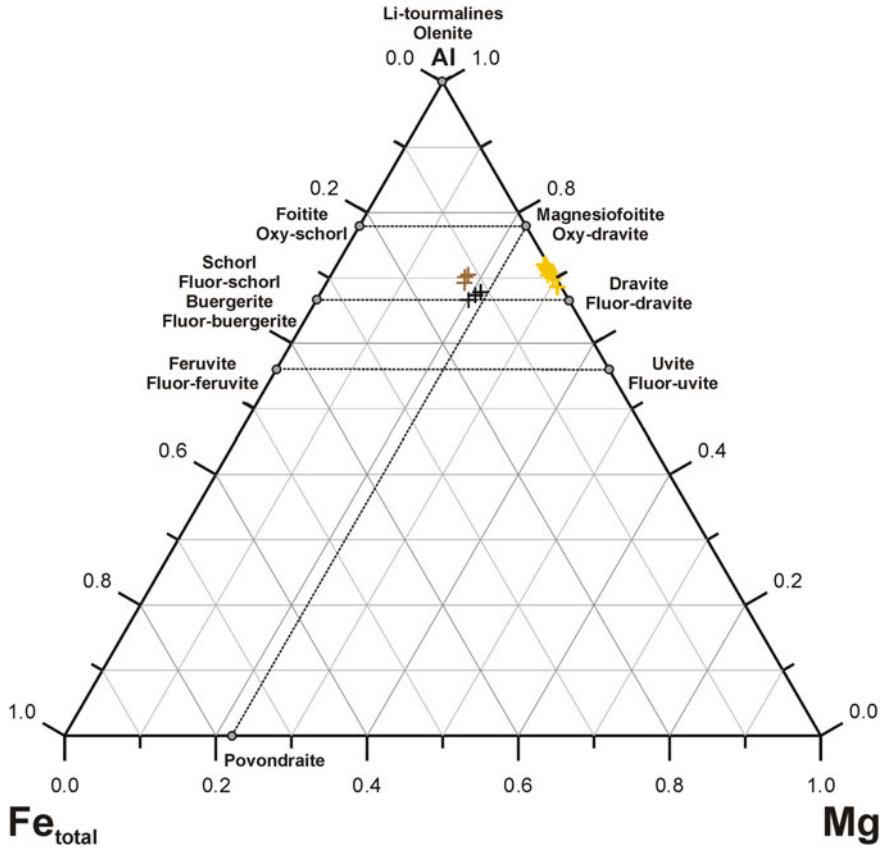

FIG. 6. Compositions of the Wołowa Góra Mountain dravitic tourmalines in the ternary system Mg–Al–Fe_{total}. Symbols as in Fig. 4.

$(BO_3)_3(OH)_3O$. The equation formally provides an opportunity to evaluate the degree of the disordering from the microprobe results, because, according to Hawthorne (1996), the $^{W}O^{2-}$ content should be equal to the smaller of the two quantities: ^{Y}Al/2 or ^{Z}Mg. However Bosi (2011), based on analysis of short-range constraints in the tourmaline structure, demonstrated that the smaller of two values $^{Y}R^{3+}/2$ and $^{Z}R^{2+}$ may not match the content of oxygen at the *W* site.

The application of the short-range constraints for yellowish dravite Trm_i predominated with the oxy-dravitic component indicates that for $^{W}O^{2-}$ = 0.46(8) apfu (average; Table 1), the ^{Y}(Al + Ti + V) content should range between 1.26–1.58 apfu, with the mean content of 1.42 apfu (in the calculation Ti^{4+} was treated along with trivalent octahedral cations Al^{3+} and V^{3+}). For the secondary fluor-dravite–fluor-schorl and dravite–schorl tourmalines Trm_{ii} and Trm_{iii}, with $^{W}O^{2-}$ of 0.29(5) and 0.29(3) apfu, the predicted mean ^{Y}(Al + Ti) contents are equal to 1.07 apfu. The values suggest the following populations at the *Y* and *Z* sites of the tourmalines:

Trm_i: $^{Y}(Mg_{1.53}Al_{1.35}Ti_{0.06}Fe^{2+}_{0.04}V_{0.01})_{\Sigma3}$ $^{Z}(Al_{4.98}Mg_{1.02})_{\Sigma6}\cdots{}^{W}[O_{0.46}F_{0.21}(OH)_{0.33}]_{\Sigma1}$

Trm_{ii}: $^{Y}(Mg_{0.86}Fe^{2+}_{1.07}Al_{1.01}Ti_{0.06})_{\Sigma3}$ $^{Z}(Al_{5.24}Mg_{0.76})_{\Sigma6}\cdots{}^{W}[F_{0.46}O_{0.29}(OH)_{0.25}]_{\Sigma1}$

Trm_{iii}: $^{Y}(Mg_{0.85}Fe^{2+}_{1.07}Al_{0.95}Ti_{0.12})_{\Sigma3}$ $^{Z}(Al_{5.02}Mg_{0.98})_{\Sigma6}\cdots{}^{W}[F_{0.39}(OH)_{0.35}O_{0.27}]_{\Sigma1}$

Crystal structure of the primary tourmaline with a predominant oxy-dravite component

The total number of the electrons in the *X*, *Y*, *Z*, *B* and *T* sites derived from structural analysis, 225.1 (0.4) e^-, corresponds within 1 standard deviation

(SD) range to the number of electrons derived from the average chemical composition of the tourmaline, 225.4(1.2) e^- (Table 1*b*). The *B* site is occupied only with boron, as the refined mean bond length <*B*–O> = 1.374(1) Å is compatible with a distance of 1.374(2) Å evaluated by Bosi and Lucchesi (2007) for tourmalines with the site completely filled with B^{3+}. Similarly the *T* site, although showing the shortened <*T*–O> distance of 1.617(1) Å, is filled only with Si. An average *T*–O distance significantly below 1.620 Å can indicate the presence of tetrahedrally-coordinated B^{3+} substituted for Si, however, a preliminary refinement with a released *T*-site occupancy showed no significant amounts of ^{IV}B. Bosi and Lucchesi (2007) proposed a reliable and statistically significant value of <Si–O> = 1.619(1) Å for the *T* site fully occupied by silicon, which is, within the standard deviation, identical to our measured <*T*–O> distance. The refined *X*-site scattering, corresponding to 0.744(7) Na + 0.120 Ca apfu, agrees within 1 sd with an occupancy of the site by 0.75(6) Na + 0.12(6) Ca apfu (Table 1). Both the refined *Z*-site scattering equal to 77.4 e^- as well as the extended <*Z*–O> distance up to 1.9247 (7) Å indicate Mg-Al disorder among the *Y* and *Z* sites. Along with the *W*-site occupation, $O_{0.46}OH_{0.33}F_{0.21}$, all the results describe the disordered distribution of ions in the structure of this tourmaline, which is characteristic for a tourmaline predominant with the oxy-dravite component. As there is only 1 e^- difference between Mg and Al, the ^{Z}Mg content was estimated as 0.64(2) apfu through intersection of the refined <*Z*–O> distance using the variation in <*Z*–O> as a function of the $^{Z}(Al + Fe^{3+})$ content presented by Lussier *et al*. (2016). Ferrous iron was refined at the *Y* site with the content of 0.153(9) apfu. The content agrees with the sum of Ti + Fe + V = 0.12(2) apfu in the mean chemical composition. The ^{Y}Mg and ^{Y}Al contents were estimated on the basis of the *Y*-site scattering, 38.14(13) e^-, diminished by 2.78 e^-, i.e. the total electron number for 0.06Ti + 0.04Fe + 0.01 V apfu. The difference of 3 apfu at the *Y* site gives ^{Y}Mg and ^{Y}Al scattering of 35.36(13) e^- and leads to the following population of the *Y* triad: $(Mg_{2.11}Al_{0.78}Ti_{0.06}Fe_{0.04}V_{0.01})_{\Sigma3}$. The population agrees within ~1.0 SD of the refined *Y*-site scattering with the *Y*-site population estimated as the difference between the total numbers of Al and Mg and the evaluated *Z*-site population. Finally, the structural formula of Trm_i tourmaline from Wołowa Mountain, with a significant oxy-dravite component, can be presented as $(Na_{0.75}Ca_{0.12}\square_{0.13})_{\Sigma1}(Mg_{1.93}Al_{0.95}Ti_{0.06}Fe^{2+}_{0.04}V_{0.01})_{\Sigma3}(Al_{5.38}Mg_{0.62})_{\Sigma6}B_3Si_6O_{27}(OH)_3(O_{0.46}OH_{0.33}F_{0.21})_{\Sigma1}$.

Origin

In the petrological diagrams of Henry and Guidotti (1985), showing the relationships between the composition of a tourmaline and its parent-magmatic or metamorphic rock, the Wołowa Góra dravitic tourmalines plot in terms of Al, Fe and Mg in the fields of aluminous metapelites and metapsammites, low-Ca ultramafics and (Cr,V)-rich metasediments (Fig. 7). Occurrences of V- and Cr-poor or -free oxy-dravite are linked mainly to quartz-mica schists (Bosi and Skogby, 2013), mica schists (Henry and de Brodtkorb, 2009; Čopjakova *et al*., 2012), cordierite-bearing schists (Redler *et al*., 2016), and metamorphosed evaporite cap rocks (Henry *et al*., 1999; Žáček *et al*., 2000), whereas its Cr- and V-bearing varieties are linked to black shales, calcareous metasediments and graphite quartzites (e.g. Bosi and Lucchesi, 2004; Bačik *et al*., 2011; Cempírek *et al*., 2013). In the case of Wołowa Mountain, the primary dravite associated with secondary fluor-dravite/fluor-schorl and dravite/schorl tourmalines, occurs within a small quartz vein (a silica-bearing mobilizate) hosted in granitic gneisses of the Kowary unit, adjacent (within a distance of a dozen to a few hundred metres) to chlorite-mica schists, quartzo-feldspathic schists and amphibolites that form the Skalny Stół massif with Czoło Mountain and Wołowa Mountain (Fig. 1). The well-known amphibolites from the nearby Budniki area, have an alkali-basalt character and correspond to recent within-plate basalts (Oberc-Dziedzic *et al*., 2010). They contain disseminated Ti mineralization in the form of rutile–ilmenite–titanite aggregates several millimetres in size, and trace sulfide mineralization composed of pyrrhotite, pentlandite, gersdorffite, cobaltite, arsenopyrite, pyrite, chalcopyrite, sphalerite, galena, marcasite, and traces of wolframite and scheelite (Mochnacka *et al*., 2008). Along with the quartzo-feldspathic schists they are considered differentiation products of a Late Cambrian to Early Ordovician bimodal volcanism with basic lavas and tuffs, acidic tuffs and intercalations of acidic and basic tuffs deposited as a volcano-sedimentary succession very probably during the ~500 Ma intense magmatic activity. The suite is interpreted as the magmatic products of Cambro–Ordovician rifting processes at a passive continental margin (Oberc-Dziedzic *et al*., 2010 and references

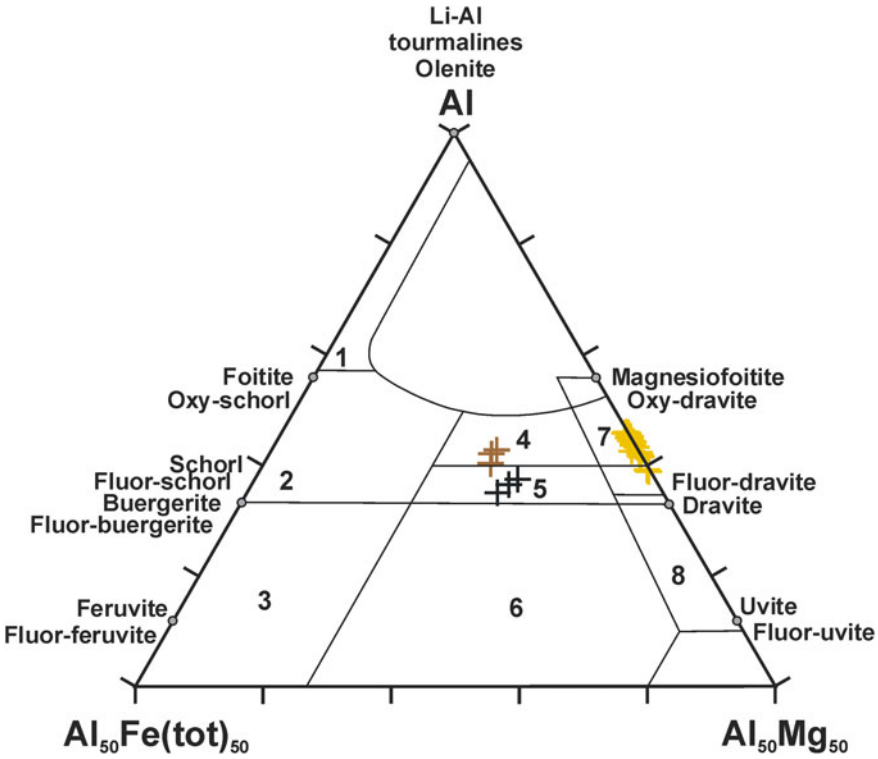

FIG. 7. Plot of the Wołowa Góra Mountain Mg-rich tourmalines in the petrogenetic Mg–Al–Fe_{total} diagram of Henry and Guidotti (1985). Description of the fields: 1 – Li-rich granitoid pegmatites and aplites; 2 – Li-poor granitoids, pegmatites and aplites; 3 – Fe-rich quartz-tourmaline rocks (hydrothermally-altered granitic rocks); 4 – Al-rich metapelites and metapsammites; 5 – Al-poor metapelites and metapsammites; 6 – Fe^{3+}-rich quartz-tourmaline rocks; calc-silicates and metapelites; 7 – low-Ca ultramafics and (Cr,V)-rich metasediments; 8 – metacarbonates and metapyroxenites.

therein). Furthermore, all the rocks underwent Early Variscan regional metamorphism (360–340 Ma; 550–600°C, P ~6 kbar), and younger contact metamorphism (325–310 Ma; 540–635–470°C) induced by the Variscan intrusion of the Karkonosze granite (Mochnacka *et al*., 2008; Oberc-Dziedzic *et al*. 2010 and references therein).

Textural and compositional relationships observed for the yellow dravitic tourmaline indicate that oxy-dravite is its basic component, carrying traces of V, which is also present in the chemical compositions of rutile, ilmenite and titanite in the nearby Budniki area (Mochnacka *et al*., 2008). Thus, it is most likely that this tourmaline was grown from an Al- and Mg-rich protolith, which could have been derived from a highly metasomatically altered prior protolith, most probably related to the silicic volcaniclastic material of the bimodal volcanism. During the regional metamorphism, the protolith released a (H_2O,B,F)-bearing fluid, which mobilized the most soluble components (mainly SiO_2 and some other oxides) and propagated them into the surrounding rocks, leading to the crystallization of a Mg-rich tourmaline (with a significant oxy-dravite component) in quartz veins. Fluor-dravite and dravite, two secondary tourmalines crystallized during a hydrothermal overprint that can be related to later stages of the regional metamorphism, or even early stages of the contact metamorphism. Such late growth in the form of elongate zones and termination zones is usually associated with a late influx of B-bearing fluids that initiate nucleation of a new tourmaline on the fracture surface or partially replacing the earlier tourmaline generation (e.g. Henry *et al*., 2002). An influx of late B-bearing fluid satisfactorily explains the enrichment in Fe, and also in Ca and Ti of the secondary fluor-dravite and schorl-dravite in relation to the primary (oxy-)dravite as a result of a few stages of partial decomposition and recrystallization of amphiboles, plagioclases and Ti-bearing

minerals present in the nearby Budniki area, and remobilization of Ca^{2+}, Ti^{4+} and Fe to the fluids at elevated temperature (Mochnacka *et al.*, 2008). This also explains why in the quartz vein from Wołowa Mountain oxy-dravite is a rare tourmaline, found only in the form of relics – small accumulations of the primary unaltered metamorphic dravite–oxy-dravite in inner parts of the vein. In the outer part of the vein, the tourmaline that was affected strongly by the fluids changed into the dominant dark green fluor-dravite/fluor-schorl and schorl-dravite, and black schorl in the host gneisses.

The yellowish colour of the primary Mg-rich tourmaline and yellowish-olive-brown colour observed in the secondary tourmaline varieties result from varying amounts of Fe^{2+} and Ti^{4+} in these tourmalines. The Fe/Ti ratio ranges from very low values of 0.4–1.7 in the primary tourmaline, through 17–19 in the secondary tourmalines from transverse veinlets, to 9–11 in the crystal's termination. In accordance with the spectroscopic data of Mattson and Rossman (1988) and da Fonseca-Zang *et al.* (2008), these data suggest that the colouration is mainly a result of the Fe^{2+}–Ti^{4+} charge-transfer transitions. The transitions are responsible for the absorption at ~24,000 cm^{-1} and the yellowish-brown to brown colour. In the primary tourmaline, the Fe content is tiny and the probability of the Fe^{2+}–Ti^{4+} charge-transfer transition is very small, which even at a relatively high $Ti^{4+}(d^0)$ content only results in yellowish colouration. The increase of Fe^{2+} in the secondary tourmalines elevates the probability of the Fe^{2+}–Ti^{4+} transitions and absorption at ~24,000 cm^{-1}; however, an absorption at ~14,000 cm^{-1} appears simultaneously which is responsible for a blue colour, originating mainly from the spin-allowed crystal-field transitions of Fe^{2+} (Mattson and Rossman, 1988; da Fonseca-Zang *et al.*, 2008). The colouration of greenish tints is a superposition of both types of absorptions, and may occur at relatively high contents of Fe^{2+} and elevated Ti^{4+}.

The presence of oxy-dravite in stratiform layers of tourmalinites hosted in mica schists was also noted in the southern, Czech part of the Kowary–Izera unit (Čopjakova *et al.*, 2012). This oxy-dravite tourmaline, associated with dravite + schorl and foitite + magnesiofoitite, has also been characterized by high values of the Mg/(Mg + Fe) ratio of 0.81–0.99, and comparable contents of Na (0.59–0.85 apfu), Ca (0.03–0.19 apfu) and *X*-site vacancy (0.04–0.39 apfu) as well as calculated $^{W}O^{2-}$ (0.25–0.87 apfu), resulting in a slightly higher average content of the oxy-dravitic component (53 mol.%). However, this oxy-dravitic tourmaline was interpreted as pre-metamorphic, formed during the interaction of an Al- and Mg-rich volcano-sedimentary protolith with B-rich fluids, and the later schorl-dravite tourmaline was interpreted to be metamorphic.

Conclusions

Yellowish dravitic tourmaline, occurring in a quartz vein hosted by gneisses of the Kowary unit on the pass between Wołowa Mountain and Czoło Mountain in the main Karkonosze range, SW Poland, represents the dravite species with a dominant oxy-dravite component. Crystals of the tourmaline are cross-cut, and in the fissures fluor-dravite/fluor-schorl grading into dravite/schorl crystallized as secondary tourmaline varieties. All the tourmalines have a metamorphic origin. The primary dravite grading into oxy-dravite formed during Variscan prograde metamorphism under the action of a released (H_2O,B,F)-bearing fluid, which mobilized the most soluble components of the altered silicic volcaniclastic material of the Late Cambrian to Early Ordovician bimodal volcanism as protholiths for adjacent quartzo-feldspathic schists and amphibolites, and propagated them into the surrounding gneisses of the Kowary unit. Fluor-dravite and dravite, both tourmalines enriched in Fe, Ca and Ti, crystallized in the later stages of regional metamorphism, or even early stages of contact metamorphism caused by the intrusion of the Karkonosze granite, associated with the partial decomposition and recrystallization of amphiboles, plagioclases and Ti-bearing minerals and remobilization of the elements, which is observed in the host amphibolite. The primary dravitic tourmaline is characterized by: (1) extremely high predominance of Mg over Fe [Mg/(Mg + Fe) = 0.97–0.99]; (2) $^{W}O^{2-}$ contents reaching ~0.59 apfu, resulting in the dominance of the oxy-dravitic component over other tourmaline end-member species (fluor-dravite, dravite, magnesio-foitite, uvite, fluor-uvite); and (3) Mg–Al disorder between the octahedral *Y* and *Z* sites on the order of ~0.64 apfu, corroborated by the increased <*Z*–O> distance up to ~1.925 Å and the measured unit-cell parameters $a = 15.916(1)$ Å and $c = 7.180(1)$ Å.

Acknowledgements

We thank the reviewers Ferdinando Bosi, Darrel J. Henry and Peter Leverett, and the Principal Editor

Peter Williams for constructive comments on this manuscript. The studies were supported by the AGH UST grant no. 11.11.140.158 to AP and by the Austrian Science Fund (FWF) projects no. P 26903-N19 and P 31049-N29 granted to AE, and by the National Science Centre (Poland) grant 2017/27/N/ST10/01579 to MS.

Supplementary material

To view supplementary material for this article, please visit https://doi.org/10.1180/minmag.2017.081.069.

References

Bačík, P., Méres, Š. and Uher, P. (2011) Vanadium-bearing tourmaline in metacherts from Chvojnica, Slovak Republic: crystal chemistry and multistage evolution. *The Canadian Mineralogist*, **49**, 195–206.

Baksheev, I.A., Prokofev, V.Yu., Yapaskurt, V.O., Vigasina, M.F., Zorina, L.D. and Solovev, V.N. (2011) Ferric-iron-rich tourmaline from the Darasun gold deposit, Transbaikalia, Russia. *The Canadian Mineralogist*, **49**, 263–276.

Berg, G. (1923) Die Gesteine des Isergebirges. *Jahrbuch der Preussischen Geologischen Landes-Anstalt, Berlin*, **43**, 125–168.

Bosi, F. (2011) Stereochemical constraints in tourmaline: from a short-range to a long-range structure. *The Canadian Mineralogist*, **49**, 17–27.

Bosi, F. and Lucchesi, S. (2004) Crystal chemistry of the schorl–dravite series. *European Journal of Mineralogy*, **16**, 335–344.

Bosi, F. and Lucchesi, S. (2007) Crystal chemical relationships in the tourmaline group: structural constraints on chemical variability. *American Mineralogist*, **92**, 1054–1063.

Bosi, F. and Skogby, H. (2012) Oxy-dravite, IMA 2012-004a. CNMNC Newsletter No. 14, October 2012, page 1285; *Mineralogical Magazine*, **76**, 1281–1288.

Bosi, F. and Skogby, H. (2013) Oxy-dravite, $Na(Al_2Mg)(Al_5Mg)(Si_6O_{18})(BO_3)_3(OH)_3O$, a new mineral species of the tourmaline supergroup. *American Mineralogist*, **98**, 1442–1448.

Bosi, F., Reznitskii, L. and Skogby, H. (2012) Oxy-chromium-dravite, $NaCr_3(Cr_4Mg_2)(Si_6O_{18})(BO_3)_3(OH)_3O$, a new mineral species of the tourmaline supergroup. *American Mineralogist*, **97**, 2024–2030.

Bosi, F., Reznitskii, L.Z and Sklyarov, E.V. (2013*a*) Oxy-vanadium-dravite, $NaV_3(V_4Mg_2)(Si_6O_{18})(BO_3)_3(OH)_3O$, crystal structure and redefinition of the "vanadium-dravite" tourmaline. *American Mineralogist*, **98**, 501–505.

Bosi, F., Skogby, H., Hålenius, U. and Reznitskii, L. (2013*b*) Crystallographic and spectroscopic characterization of Fe-bearing chromo-alumino-povondraite and its relations with oxy-chromium-dravite and oxy-dravite. *American Mineralogist*, **98**, 1557–1564.

Bosi, F., Reznitskii, L., Skogby, H. and Hallenius, U. (2014*a*) Vanadio-oxy-chromium-dravite, $NaV_3(Cr_4Mg_2)(Si_6O_{18})(BO_3)_3(OH)_3O$, a new mineral species of the tourmaline supergroup. *American Mineralogist*, **99**, 1155–1162.

Bosi, F., Skogby, H., Reznitskii, L. and Hallenius, U. (2014*b*) Vanadio-oxy-dravite, $NaV_3(Al_4Mg_2)(Si_6O_{18})(BO_3)_3(OH)_3O$, a new mineral species of the tourmaline supergroup. *American Mineralogist*, **99**, 218–224.

Bosi, F., Reznitskii, L., Hålenius, U. and Skogby, H. (2017) Crystal chemistry of Al-V-Cr oxy-tourmalines from Sludyanka complex, Lake Baikal, Russia. *European Journal of Mineralogy*, https//doi.org/10.1127/ejm/2017/0029-2617

Cempírek, J., Houzar, S., Novák, M., Groat, L.A., Selway, J.B. and Šrein, V. (2013) Crystal structure and compositional evolution of vanadium-rich oxy-dravite from graphite quartzite at Bítovánky, Czecgh Republic. *Journal of Geosciences*, **58**, 149–162.

Čopjakova, R., Škoda, R. and Vašinová-Galiova, M. (2012) "Oxy-dravite" from tourmalinites of the Krkonoše-Jizera Crystalline Massif. *Bulletin Mineralogicko-Petrologického Oddělení Národního Muzea* (*Praha*), **20**, 37–46.

da Fonseca-Zang, W.A., Zang, J.W. and Hofmeister, W. (2008) The Ti-influence on the tourmaline colour. *Journal of the Brazilian Chemical Society*, **19**, 1186–1192.

Ertl, A., Marschall, H.R., Giester, G., Henry, D.J., Schertl, H.-P., Ntaflos, T., Luvizotto, G.L., Nasdala, L. and Tillmanns, E. (2010) Metamorphic ultra high-pressure tourmalines: Structure, chemistry, and correlations to PT conditions. *American Mineralogist*, **95**, 1–10.

Ertl, A., Baksheev, I.A., Giester, G., Lengauer, C.L., Prokofiev, V.Y. and Zorina, L.D. (2016) Bosiite, $NaFe^{3+}_3(Al_4Mg_2)(Si_6O_{18})(BO_3)_3(OH)_3O$, a new ferric member of the tourmaline supergroup from the Darasun gold deposit, Transbaikalia, Russia. *European Journal of Mineralogy*, **28**, 581–591.

Fischer, R.X. and Tillmanns, E. (1988) The equivalent isotropic displacement factor. *Acta Crystallographica* **C44**, 775–776.

Gawęda, A., Pieczka, A. and Kraczka, J. (2002) Tourmalines from the Western Tatra Mountains (W-Carpathians, S-Poland): their characteristics and petrogenetic importance. *European Journal of Mineralogy*, **14**, 943–955.

Hawthorne, F.C. (1996) Structural mechanism for light-element variations in tourmaline. *The Canadian Mineralogist*, **34**, 123–132.

Hawthorne, F.C. and Henry, D.J. (1999) Classification of the minerals of the tourmaline group. *European Journal of Mineralogy*, **11**, 201–215.

Henry, D.J. and de Brodtkorb, M.K. (2009) Mineral chemistry and chemical zoning in tourmalines, Pampa del Tamboreo, San Luis, Argentina. *Journal of South American Earth Sciences*, **28**, 132–141.

Henry, D.J. and Guidotti, C.V. (1985) Tourmaline as a petrogenetic indicator mineral: an example from the staurolite-grade metapelites of NW Maine. *American Mineralogist*, **70**, 1–15.

Henry, D.J., Kirkland, B.L., Kirkland, D.W., Novák, M. and Hawthorne, F.C. (1999) Sector-zoned tourmaline from the cap rock of a salt dome. *European Journal of Mineralogy*, **11**, 263–280.

Henry, D.J., Dutrow, B.L. and Selverstone, J. (2002) Compositional asymmetry in replacement tourmaline – an example from the Tauern Window, Eastern Alps. *Geological Materials Research*, **4**, 1–18.

Henry, D.J., Novák, M., Hawthorne, F.C., Ertl, A., Dutrow, B.L., Uher, P. and Pezzotta, F. (2011): Nomenclature of the tourmaline-supergroup minerals. *American Mineralogist*, **96**, 895–913.

Lis, J., Stępniewski, M. and Sylwestrzak, H. (1965) Brannerite and co-existing minerals in the quartz vein from Wołowa Góra Mountain Near Kowary (Sudetes). *Biuletyn Instytutu Geologicznego*, **193**, 203–223 [in Polish].

Lussier, A., Ball, N.A., Hawthorne, F.C., Henry, D.J., Shimizu, R., Ogasawara, Y. and Ota, T. (2016) Maruyamaite, $K(MgAl_2)(Al_5Mg)Si_6O_{18}(BO_3)_3(OH)_3O$, a potassium-dominant tourmaline from the ultrahigh-pressure Kokchetav massif, northern Kazakhstan: Description and crystal structure *American Mineralogist*, **101**, 355–361.

Mattson, S.M. and Rossman, G.R. (1988) Fe^{2+}-Ti^{4+} charge transfer in stoichiometric Fe^{2+}, Ti^{4+}-minerals. *Physics and Chemistry of Minerals*, **16**, 78–82.

Mazur, S., Aleksandrowski, P., Turniak, K. and Awdankiewicz, M. (2007) Geology, tectonic evolution and Late Palaeozoic magmatism of Sudetes – an overview. *Granitoids in Poland, Archivum Mineralogiae Monograph*, **1**, 59–87.

Mochnacka, K., Oberc-Dziedzic, T., Mayer, W. and Pieczka, A. (2008) Ti remobilization and sulphide/sulphoarsenide mineralization in amphibolites: effect of granite intrusion (the Karkonosze-Izera Massif, SW Poland). *Geological Quarterly*, **52**, 349–368.

Oberc-Dziedzic, T., Kryza, R., Mochnacki, K. and Larionov, A. (2010) Ordovician passive continental margin magmatism in the Central-European Variscides: U–Pb zircon data from the SE part of the Karkonosze-Izera Massif, Sudetes, SW Poland. *International Journal of Earth Sciences* (*Geologishe Rundschau*), **99**, 27–46.

Pieczka, A. (1996) Mineralogical study of Polish tourmalines. *Prace Mineralogiczne*, **85** [in Polish only].

Pieczka, A. (2007) Blue dravite from the Szklary pegmatite (Lower Silesia, Poland). *Mineralogia Polonica* **38**, 209–218.

Pieczka, A., Łobos, K. and Sachanbiński, M. (2004) The first occurrence of elbaite in Poland. *Mineralogia Polonica*, **35**, 209–218.

Pieczka, A., Gołębiowska, B. and Parafiniuk, J. (2009) Conditions of formation of polymetallic mineralization in the eastern envelope of the Karkonosze granite: the case of Rędziny, southwestern Poland. *Canadian Mineralogist*, **47**, 765–786.

Pieczka, A., Szełęg, E., Łodziński, M., Szuszkiewicz, A., Nejbert, K., Turniak, K. and Ilnicki, S. (2010) Mn-Fe fractionation in tourmalines from pegmatites in the DSS mine at Piława Górna, Góry Sowie Block, southwestern Poland (preliminary data). *Mineralogia – Special Papers*, **37**, 100.

Pieczka, A., Szuszkiewicz, A., Szełęg, E., Janeczek, J. and Nejbert, K. (2015) Granitic pegmatites of the Polish part of the Sudetes (NE Bohemian massif, SW Poland). 7th *International Symposium on Granitic pegmatites, Książ, Poland, June* 17-19, 2015. *Fieldtrip Guidebook C* 73–103.

Pouchou, I.L. and Pichoir, F. (1985) "PAP" (phi-rho-z) procedure for improved quantitative microanalysis. Pp. 104–106 in: *Microbeam Analysis* (I.T. Armstrong, editor). San Francisco Press, San Francisco, USA.

Redler, Ch., Irouschek, A., Jeffries, T. and Gieré, R. (2016) Origin and formation of tourmaline-rich cordierite-bearing metapelitic rocks from Alpe Sponda, Central Alps (Switzerland). *Journal of Petrology* **57**, 277–308.

Reznitsky, L.Z., Sklyarov, E.V., Ushapovskaya, Z.F., Nartova, N.V., Kashaev, A.A., Karmanov, N.S., Kanakin, S.V., Smolin, A.S., Nekrasova, E.A. (2001) Vanadiumdravite, $NaMg_3V_6[Si_6O_{18}][BO_3]_3(OH)_4$, a new mineral of the tourmaline group. *Proceedings of Russian Mineralogical Society* **130**, 59–72 [in Russian].

Reznitskii, L., Clark, C.M., Hawthorne, F.C., Grice, J.D., Skogby, H., Hålenius, U. and Bosi, F. (2014) Chromo-alumino-povondraite, $NaCr_3(Al_4Mg_2)(Si_6O_{18})(BO_3)_3(OH)_3O$, a new mineral species of the tourmaline supergroup. *American Mineralogist*, **99**, 1767–1773.

Różański, P. (1995) *Zdjęcie geologiczne głównego grzbietu Karkonoszy między Czołem a Czarnym Grzbietem*. MSc Theses. University of Wrocław, Poland.

Sheldrick, G.M. (1998) *SHELXL97, Release 97-2. Program for Crystal Structure Refinement*. University of Göttingen, Göttingen, Germany.

Žáček, V., Frýda, J., Petrov, A. and Hyršl, J. (2000) Tourmalines of the povondraite – (oxy)dravite series from the cap rock of meta-evaporite in Alto Chapare, Cochabamba, Bolivia. *Journal of the Czech Geological Society*, **45**, 3–12.